ORIGINAL PAPER

Physiologically-based pharmacokinetic modeling to predict drug-drug interaction of enzalutamide with combined P-gp and CYP3A substrates

Yukio Otsuka[1] · Srinivasu Poondru[2] · Peter L. Bonate[2] · Rachel H. Rose[3] · Masoud Jamei[3] ·
Fumihiko Ushigome[4] · Tsuyoshi Minematsu[5]

Abstract

Enzalutamide is known to strongly induce cytochrome P450 3A4 (CYP3A4). Furthermore, enzalutamide showed induction and inhibition of P-glycoprotein (P-gp) in in vitro studies. A clinical drug-drug interaction (DDI) study between enzalutamide and digoxin, a typical P-gp substrate, suggested enzalutamide has weak inhibitory effect on P-gp substrates. Direct oral anticoagulants (DOACs), such as apixaban and rivaroxaban, are dual substrates of CYP3A4 and P-gp, and hence it is recommended to avoid co-administration of these DOACs with combined P-gp and strong CYP3A inducers. Enzalutamide's net effect on P-gp and CYP3A for apixaban and rivaroxaban plasma exposures is of interest to physicians who treat patients for venous thromboembolism with prostate cancer. Accordingly, a physiologically-based pharmacokinetic (PBPK) analysis was performed to predict the magnitude of DDI on apixaban and rivaroxaban exposures in the presence of 160 mg once-daily dosing of enzalutamide. The PBPK models of enzalutamide and M2, a major metabolite of enzalutamide which also has potential to induce CYP3A and P-gp and inhibit P-gp, were developed and verified as perpetrators of CYP3A-and P-gp-mediated interaction. Simulation results predicted a 31% decrease in AUC and no change in C_{max} for apixaban and a 45% decrease in AUC and a 25% decrease in C_{max} for rivaroxaban when 160 mg multiple doses of enzalutamide were co-administered. In summary, enzalutamide is considered to decrease apixaban and rivaroxaban exposure through the combined effects of CYP3A induction and net P-gp inhibition. Concurrent use of these drugs warrants careful monitoring for efficacy and safety.

✉ Yukio Otsuka
yukio.otsuka@astellas.com

1 Clinical Pharmacology and Exploratory Development, Astellas Pharma Inc., 2-5-1, Nihonbashi-honcho, Chuo-ku, Tokyo 103-8411, Japan

2 Clinical Pharmacology and Exploratory Development, Astellas Pharma Global Development Inc., Northbrook, IL, USA

3 Simcyp Division, Certara UK, Sheffield, UK

4 Applied Research and Operations, Astellas Pharma Inc., Ibaraki, Japan

5 Immuno-oncology, Astellas Pharma Inc., Ibaraki, Japan

Introduction

Enzalutamide (MDV3100) is an androgen receptor (AR) inhibitor that targets the AR signaling pathway. Enzalutamide was approved in the US in 2012 under the tradename XTANDI® for the treatment of patients with metastatic castration-resistant prostate cancer (CRPC) who have previously received docetaxel. The indication for XTANDI was subsequently expanded to the treatment of metastatic CRPC and later to the treatment of CRPC. XTANDI was also approved in 2019 in the US for the treatment of metastatic castration-sensitive prostate cancer (mCSPC; also referred to as metastatic hormone-sensitive prostate cancer [mHSPC]). Worldwide, enzalutamide has been approved for the treatment of metastatic CRPC in more than 100 countries.

Oral absorption of enzalutamide, whether administered as single or multiple doses, is rapid and dose-independent. Peak concentrations of enzalutamide are generally achieved 1 to 2 h postdose in both patients and healthy subjects [1]. Enzalutamide is well absorbed (estimated bioavailability based on mass balance data ≥ 84%), an expected finding for a low extraction ratio drug that displays high permeability and is not a substrate for P-glycoprotein (P-gp) or breast cancer resistance protein (BCRP). A high-fat meal slows the rate of enzalutamide absorption, but the extent of absorption is unaffected. Enzalutamide has been administered without regard to meals in clinical studies in patients, including pivotal phase three studies. In vitro and in vivo protein binding data showed that enzalutamide is 97% to 98% bound to plasma proteins, primarily albumin. N-desmethyl enzalutamide (M2), the active metabolite of enzalutamide, is 95% to 97% bound to plasma proteins. In vitro studies show that enzalutamide is metabolized by cytochrome P450 2C8 (CYP2C8) and CYP3A4/5, both of which play a role in the formation of M2. In addition, an in vitro study showed that human carboxylesterase 1 (hCES1) is capable of catalyzing the formation of the carboxylic acid metabolite (M1) from enzalutamide and M2. Following oral administration of ^{14}C-enzalutamide to healthy male subjects, 85% of the dose was recovered through day 77 postdose: 71% was recovered in urine (primarily as M1, with trace amounts of enzalutamide and M2) and 14% was recovered in feces (0.39% as enzalutamide) [1]. Based on this information, renal excretion is considered a minor elimination pathway for unchanged parent enzalutamide and M2. With assuming all components, including M1, in metabolite profiling which possibly generated from M2 were formed from M2, M2 formation accounted for 63% of dosed enzalutamide.

The potential for enzalutamide to affect the pharmacokinetics of other drugs was assessed in in vivo phenotypic cocktail drug-drug interaction (DDI) studies. At steady state, enzalutamide is a strong CYP3A4 inducer and a moderate CYP2C9 and CYP2C19 inducer [2]. Enzalutamide did not cause clinically meaningful changes in exposure to the CYP1A2, CYP2C8, or CYP2D6 substrates. In a clinical DDI study, enzalutamide increased the AUC of digoxin, a typical P-gp substrate, by 29%, indicating the net effect of enzalutamide on P-gp is inhibition-based [3]. Clinical DDI study results with rosuvastatin, a typical BCRP substrate, showed that enzalutamide did not change the plasma exposure of rosuvastatin.

In 9% of prostate cancer patients, venous thromboembolism (VTE) with high mortality risk was reported [4]. For the treatment of VTE, anticoagulation is essential in preventing thrombosis. Direct oral anticoagulants (DOACs) as first-line agents for the treatment of VTE with cancer are recommended in the guidelines issued by the American College of Chest Physicians [5] and the American Society of Hematology [6]. Drug interactions during DOAC therapy can dramatically alter their efficacy and safety profiles. Apixaban and rivaroxaban are two DOACs, both of which are dual CYP3A and P-gp substrates. Hence, drug interactions with enzalutamide are one of the concerns in VTE treatment in prostate cancer patients [7].

This study aimed to predict the magnitude of CYP3A- and P-gp-mediated induction and inhibitory effects of enzalutamide and M2 on apixaban and rivaroxaban. The in vitro ability of enzalutamide to induce CYP enzymes and P-gp, and to inhibit P-gp, was investigated. Both in vitro and in vivo clinical data were then integrated into a physiologically-based pharmacokinetic (PBPK) model to quantitatively estimate the magnitude of exposure change in apixaban and rivaroxaban when enzalutamide is concomitantly administered at clinically relevant doses.

Methods

In vitro CYP and P-gp induction study

The in vitro potential of enzalutamide and two major metabolites, M1 and M2, to induce CYP enzymes and P-gp was investigated with freshly isolated human hepatocytes. Hepatocytes were cultured according to previously described methods [8]. Enzalutamide, M1, or M2 were treated with three concentrations (1, 10, or 100 μmol/L). As positive controls, 50 μmol/L omeprazole, 750 μmol/L phenobarbital, or 10 μmol/L rifampicin were tested. Approximately 24 h after the last treatment, hepatocytes were lysed in TRIzol® reagent and total RNA was phase-extracted from the cell lysates according to the TRIzol procedure. Single-stranded cDNA was prepared from RNA with the RT Master Mix using the AB 7900HT Fast Real Time PCR System thermocycling program. Quantitative RT-PCR was carried out in triplicate. Relative quantification measures the change in mRNA expression in a test sample relative to that in a control sample (e.g., DMSO). This method assumes that the efficiency of the target amplification and the efficiency of the endogenous control amplification are approximately equal.

The maximal fold induction (Ind_{max}) and half concentration to reach Ind_{max} ($IndC_{50}$) were determined based on the following equation:

$$Fold\,induction = 1 + \frac{(Ind_{max} - 1) \times C_t}{IndC_{50} + C_t}$$

where C_t is the test drug concentration.

In vitro P-gp inhibition study

MDR1-expressing cells (porcine kidney epithelial LLC-PK1 cells transfected with human MDR1 cDNA) was used. The MDR1-expressing cells were seeded at a density of 4×10^4 cells/insert in plates and were incubated in a CO_2 incubator (37 °C, CO_2: 5%) for 7 to 9 days to prepare cell monolayers. After the cells were pre-incubated at 37 °C for 1 h, in half of the plates, the medium in the insert chamber (i.e., the apical side) was aspirated and replaced with 100 µL of test solutions, which incorporated 1 µmol/L of ^{3}H-digoxin and enzalutamide (0, 0.3, 1, 3, 10, 30, and 50 µmol/L) or M2 (0, 0.1, 0.3, 1, 3, 10, and 25 µmol/L); in the other half of the plates, the media in the well (i.e., the basal side) were aspirated and replaced with 600 µL of test solution. After incubation for 4 h at 37 °C, a 70-µL aliquot of the incubation solutions was collected as the analytical sample from the opposite compartment of that spiked with test solutions (receiver compartment). The collected samples were immediately combined with 10 mL of scintillator, and the radioactivity was counted using the LSC. Permeability coefficient (P_{app}) of ^{3}H-digoxin was calculated using the following equation:

$$P_{app} \, (cm/sec) = [dQ/dt]/A/C_0$$

where dQ/dt is the transport rate (dpm/sec); A is the membrane area (cm^2); C_0 is the initial concentration (dpm/mL). The ratio of permeability coefficient (P_{app} ratio) was calculated from the basal to apical P_{app} and apical to basal P_{app} according to the following equation:

$$P_{app} \text{ ratio} = \frac{\text{Basal to apical } P_{app}}{\text{Apical to basal } P_{app}}$$

Furthermore, the ratios of the P_{app} ratios in MDR1-expressing cells to the P_{app} ratios in control cells were calculated as corrected P_{app} ratio according to the following equation:

$$\text{Corrected } P_{app} \text{ ratio} = \frac{P_{app} \text{ ratio of the MDR1 expressing cells}}{P_{app} \text{ ratio of the control cells}}$$

The % of control was calculated from the corrected P_{app} ratio according to the following equation:

$$\% \text{ of control} =$$
$$\frac{\text{Corrected } P_{app} \text{ ratio in the absence or presence of inhibitors}}{\text{Corrected } P_{app} \text{ ratio in the absence of inhibitors}} \times 100$$

The IC_{50} value was calculated by the least squares method from the relationship between enzalutamide or M2 concentration and the % of control according to the following equation:

$$\frac{R_i}{R_a} = (1 - \frac{I_{max} \times I^C}{I^C + IC_{50}{}^C}) \times 100$$

where R_i and R_a are the corrected P_{app} ratio in the presence and absence of enzalutamide or M2, respectively; I_{max} is the maximum inhibitory effect; I is the concentration of enzalutamide or M2; and C is the Hill factor.

PBPK model development and verification

The PBPK models for enzalutamide and M2 were developed within the Simcyp Simulator version 19 (Certara UK Limited, Sheffield, UK). The advanced dissolution, absorption, and metabolism (ADAM) model for absorption and the full PBPK model for distribution were used for enzalutamide, and the minimum PBPK distribution model was used for M2.

Many of the physicochemical properties and plasma protein binding data were obtained internally and also referenced from FDA documents [9], which are available from the FDA website. The cLog P of M2 was calculated in silico (ACD/Labs percepta 14.3.0, Build 3063, Advanced Chemistry Development Inc., Toronto, Canada). The enzalutamide model was constructed for a liquid-filled capsule formulation. Accordingly, the solution formulation option in the Simcyp model was used. Permeability ($P_{eff,man}$) was predicted from Caco-2 passive permeability data, including calibration of enzalutamide permeability to the measured permeability of the propranolol as a reference. The volume of distribution was predicted using the Simcyp built-in methods (Method 2 for enzalutamide and Method 1 for M2) with slight modification in enzalutamide using the K_p scalar to obtain clinically observed volume of distribution [9]. An in vitro study suggested enzalutamide was metabolized by CYP3A4 and CYP2C8 forming M2 [2]. From the clinical mass balance and metabolite profiling data, 63% of dosed enzalutamide was metabolized to M2. The contribution of CYP2C8 and CYP3A4 to the formation of M2 was estimated from a clinical DDI study result using gemfibrozil, a strong CYP2C8 inhibitor, as the perpetrator. The elimination pathway of M2 is not known; however, concomitant administration of itraconazole, a strong CYP3A4 inhibitor, increased AUC_{inf} of M2 in the clinical DDI study [2], indicating possible contribution of CYP3A4 to the elimination of M2. The CYP3A4 contribution to M2 elimination was determined from exposure after multiple-dose administration of enzalutamide, which was possibly affected with autoinduction of CYP3A4. The ability of the enzalutamide and M2 PBPK models to predict CYP3A induction was confirmed using a DDI simulation with midazolam as the victim. The net effect of enzalutamide on P-gp was investigated in a clinical DDI study using digoxin as a typical P-gp substrate [3]. Enzalutamide inhibition and induction effects to P-gp were optimized based on the results from a clinical DDI study.

The PBPK models of CYP2C8 inhibitor (gemfibrozil), CYP3A4 substrate (midazolam), and P-gp substrate (digoxin) were used from the Simcyp software library with models that were verified for their intended purpose.

Application to DDI simulation

The DDI prediction of enzalutamide with apixaban and rivaroxaban (CYP3A and P-gp substrates) in a cancer population was performed in 100 virtual subjects. The PBPK models for apixaban and rivaroxaban were previously developed and verified for CYP3A- and P-gp-mediated interaction [10]. Two models for rivaroxaban, one considered OAT3 involvement in renal elimination (Model 1) and one did not (Model 2), were reported. Accordingly, the rivaroxaban DDI was investigated for both these models. Sensitivity analysis was conducted on the influence of intestinal P-gp activities of apixaban and rivaroxaban on the DDI with enzalutamide. P-gp relative activity factor/relative expression factor (RAF/REF) is used to scale in vitro to in vivo activity by multiplying RAF/REF to in vitro P-gp intrinsic clearance ($CL_{int,p-gp}$; apixaban) or maximal rate of P-gp-mediated drug transport (J_{max}; rivaroxaban). During the model development process, intestinal P-gp activity was adjusted by modifying the P-gp RAF/REF values. Accordingly, a sensitivity analysis was performed to assess the impact of these changes on the predicted magnitude of the DDI.

Results

In vitro CYP and P-gp induction and P-gp inhibition studies

In the CYP and P-gp induction study, there was a tendency that the increases in mRNA expression were highest following treatment with enzalutamide 10 μmol/L not the highest drug concentration tested, 100 μmol/L (Table 1).

Of the CYP isozymes tested, CYP3A4 showed the greatest increase following enzalutamide or M2 treatment, with up to a 6.90-fold increase (95.9% of positive control) in mRNA levels being observed, on average. In contrast, CYP1A2 did not show an increase in mRNA levels, while the other CYP isozymes (CYP2B6, CYP2C8, CYP2C9, and CYP2C19) showed some small increases in mRNA levels. For P-gp mRNA expression levels, treatment with 10 μmol/L enzalutamide or M2 caused a 2.16- and 1.66-fold increase, respectively, on average. The Ind_{max} and $IndC_{50}$ for CYP3A4 were determined as 5.9-fold and 1.5 μmol/L, respectively, for enzalutamide and 5.1-fold and 2.5 μmol/L, respectively, for M2. When input to the Simcyp simulator, Ind_{max} was calibrated with positive

control, rifampicin, and the calibrated values were 11.43 and 9.72 for enzalutamide and M2, respectively. M1 showed only minor effects on CYP enzymes and P-gp mRNA expression levels.

In the P-gp inhibition study, the corrected P_{app} ratio of ^{3}H-digoxin across MDR1-expressing cells was decreased when co-incubated with increasing enzalutamide or M2 concentrations (Table 2).

The IC_{50} values were estimated to be 1.67 and 1.09 μmol/L for enzalutamide and M2, respectively. The concentration of digoxin was set smaller than its K_m value and determined IC_{50} values were regarded as inhibition constant (K_i) in the DDI simulation. M1 did not inhibit P-gp-mediated ^{3}H-digoxin transport.

PBPK model development and verification of enzalutamide and M2

Based on the clinical DDI study result with gemfibrozil, the contribution of CYP2C8 on enzalutamide elimination was estimated to be 87%, with the remaining percent assigned to CYP3A4-mediated metabolism. Further, setting 67% of CYP2C8 CL_{int} to M2 formation and the remaining 33% to other pathways allowed recovery of the M2 AUC ratio. To maintain conversion of enzalutamide to M2 at 63%, the fraction of CYP3A4 CL_{int} contributing to M2 formation was set at 39% and the remaining 61% of CYP3A4 CL_{int} was assigned to other pathways. In the assignment of M2 elimination pathway, CYP3A4 contribution of 9% resulted in recovery of M2 exposure after multiple doses of enzalutamide. For the enzalutamide model, the CL_{int} of each pathway was calculated from the CL_{po} of 0.60 L/h observed in a food effect study using the retrograde calculation method in the Simcyp simulator (Table 3).

The predictability of plasma concentration–time profiles (Fig. 1) and PK parameters (Table S1, Table S2) was confirmed after single and multiple oral administration of enzalutamide in clinical studies. The datasets are independent from enzalutamide model development, except for M2 concentration data after multiple doses were used for the determination of CYP3A4 contribution in hepatic metabolism of M2. The developed enzalutamide and M2 models showed good reproducibility of the plasma concentration–time profiles when 160 mg enzalutamide was administered once, or multiple times (Fig. 1).

Further, the model capability to simulate enzalutamide plasma concentrations after single- and multiple-dose administration at several dose levels was confirmed (Fig. 2).

Due to autoinduction of CYP3A4, both the capability of the model to capture multiple-dose clinical data and the DDI simulation result with midazolam confirmed the

Table 1 The effects of treating culture human hepatocytes with enzalutamide, M2, or prototypical inducers on CYP and P-gp mRNA levels

Treatment	Conc. (μmol/L)	Fold increase						
		CYP1A2	CYP2B6	CYP2C8	CYP2C9	CYP2C19	CYP3A4	P-gp
Enzalutamide	1	1.14 ± 0.53	1.50 ± 0.45	2.14 ± 0.74	1.41 ± 0.27	1.07 ± 0.15	2.24 ± 0.82	1.17 ± 0.07
Enzalutamide	10	1.06 ± 0.23	3.36 ± 0.72	10.9 ± 5.2	3.28 ± 0.71	1.92 ± 1.22	6.90 ± 2.25	2.16 ± 0.29
Enzalutamide	100†	0.333	2.34	3.12	1.10	1.26	4.62	1.74
Ind$_{max}$		–	–	–	–	–	5.9	–
IndC$_{50}$		–	–	–	–	–	1.5	–
M1	1	0.697 ± 0.260	0.724 ± 0.316	1.11 ± 0.53	0.853 ± 0.361	0.855 ± 0.246	0.832 ± 0.417	0.885 ± 0.553
M1	10	0.883 ± 0.303	1.03 ± 0.43	1.44 ± 0.50	0.888 ± 0.172	1.06 ± 0.10	1.17 ± 0.46	1.46 ± 0.79
M1	100	1.01 ± 0.59	0.848 ± 0.337	2.35 ± 1.66	1.52 ± 0.63	1.55 ± 0.80	1.83 ± 0.98	1.32 ± 0.25
M2	1	0.561 ± 0.100	0.705 ± 0.208	1.73 ± 1.10	1.00 ± 0.27	0.872 ± 0.205	1.42 ± 0.31	0.894 ± 0.513
M2	10	0.960 ± 0.279	1.96 ± 0.14	7.40 ± 3.26	2.38 ± 0.48	1.18 ± 0.46	5.30 ± 2.77	1.66 ± 0.61
M2	100†	0.842	1.80	8.93	1.50	2.12	4.32	1.63
Ind$_{max}$		–	–	–	–		5.1	–
IndC$_{50}$		–	–	–	–		2.5	–
Omeprazole	50	46.4 ± 7.2	–	–	–	–	–	2.38 ± 1.68
Phenobarbital	750	–	6.90 ± 3.66	–	–	–	–	2.61 ± 0.59
Rifampicin	10	–	–	14.0 ± 5.6	3.64 ± 0.47	3.80 ± 3.61	8.05 ± 4.10	3.60 ± 2.30

Data were expressed as mean ± SD from three lots of hepatocyte

†data for 100 μmol/L were obtained from two lots of hepatocyte

developed models were verified for modelling CYP3A induction effects in clinical aplications (Table 4).

Furthermore, the enzalutamide and M2 models were optimized to simulate net effects on P-gp. Among the tested P-gp induction by enzalutamide, fold-increase in P-gp expression of 1.0 (no induction) resulted in the closest AUC ratio to observed (Table 4, Fig. 3).

DDI simulation with apixaban and rivaroxaban

The DDI simulation with apixaban and rivaroxaban was performed under the assumption of no P-gp induction effect (P-gp fold increase of 1.0) of enzalutamide and M2 in the models. After single oral administration of 10 mg of apixaban with 160 mg of enzalutamide after 50 days of multiple oral administrations, a 31% decrease in AUC and no change in C_{max} were predicted (Table 5).

After single oral administration of 20 mg of rivaroxaban with 160 mg of enzalutamide after 50 days of multiple oral administrations, a 45% and 42% decrease in AUC and a 25% and 23% decrease in C_{max} were simulated in Model 1 (with OAT3 model) and Model 2 (without OAT3 model), respectively. Sensitivity analysis of intestinal P-gp activity on enzalutamide's effect on apixaban and rivaroxaban exposure was tested. With apixaban, AUC and C_{max} ratios ranged from 0.651 to 0.815 and from 0.916 to 1.25, respectively, for the tested intestinal P-gp RAF/REF of 2.5 to 100 (default 25). With rivaroxaban, AUC and C_{max} ratios ranged from 0.561 to 0.619 and from 0.711 to 0.801, respectively, for the tested intestinal P-gp RAF/REF of 0.015 to 0.60 (default 0.15).

Discussion

Enzalutamide and M2 PBPK models were developed and verified to be used for predicting DDI with CYP3A substrates and P-gp substrates. The plasma concentration profiles of enzalutamide and M2 were simulated using the developed PBPK models, giving similar profiles to those clinically observed after single and multiple doses. The simulation results well captured the observed plasma concentration profiles of enzalutamide and M2, except for C_{max} of parent after single-dose administration of enzalutamide (Fig. 1, Table S1). The simulated C_{max} of enzalutamide after single-dose administration was 40% lower than observed; however, after multiple-dose simulation, simulated AUC, C_{max}, and C_{min} are close to those observed and underestimation in C_{max} after a single dose was considered not to influence the DDI simulation. Although enzalutamide and M2 showed induction effects on CYP2C8 in an in vitro study, a clinical DDI study with a sensitive CYP2C8 substrate, pioglitazone, indicated enzalutamide did not cause a clinically meaningful interaction

Table 2 Inhibitory effect of enzalutamide on ^{3}H-digoxin (1 μmol/L) permeation across control and MDR1-expressing cell monolayers

Additive	Concentration (μmol/L)	Control cells			MDR1-expressing cells			Corrected P_{app} ratio	IC_{50} (μmol/L)
		P_{app} (× 10^{-6} cm/sec)		P_{app} ratio	P_{app} (× 10^{-6} cm/sec)		P_{app} ratio		
		A to B	B to A		A to B	B to A			
Enzalutamide	0	1.73 ± 0.73	1.66 ± 0.06	1.0	0.641 ± 0.028	12.8 ± 0.6	20.0	20.0	1.67
	0.3	1.39 ± 0.20	1.85 ± 0.31	1.3	0.725 ± 0.043	12.4 ± 0.8	17.1	13.2	
	1	1.47 ± 0.14	1.94 ± 0.13	1.3	0.851 ± 0.081	13.4 ± 0.4	15.7	12.1	
	3	1.68 ± 0.13	2.02 ± 0.10	1.2	1.25 ± 0.26	12.1 ± 0.9	9.7	8.1	
	10	2.09 ± 0.07	2.20 ± 0.10	1.1	1.41 ± 0.08	11.0 ± 0.6	7.8	7.1	
	30	2.42 ± 0.24	2.56 ± 0.19	1.1	2.11 ± 0.09	7.85 ± 0.28	3.7	3.4	
	50	2.22 ± 0.21	2.63 ± 0.32	1.2	2.73 ± 0.12	7.22 ± 0.18	2.6	2.2	
M1	0	1.39 ± 0.09	1.66 ± 0.23	1.2	0.683 ± 0.105	15.6 ± 1.2	22.8	19.0	–
	0.3	1.22 ± 0.06	1.62 ± 0.22	1.3	0.807 ± 0.032	13.8 ± 1.1	17.1	13.2	
	1	1.31 ± 0.06	1.62 ± 0.03	1.2	0.670 ± 0.029	14.0 ± 1.2	20.9	17.4	
	3	1.39 ± 0.05	1.44 ± 0.13	1.0	0.725 ± 0.011	13.9 ± 0.4	19.2	19.2	
	10	1.36 ± 0.11	1.36 ± 0.12	1.0	0.626 ± 0.033	13.6 ± 1.0	21.7	21.7	
	30	1.43 ± 0.06	1.46 ± 0.13	1.0	0.715 ± 0.045	13.1 ± 0.4	18.3	18.3	
	80	1.43 ± 0.10	1.47 ± 0.13	1.0	0.623 ± 0.035	13.3 ± 0.9	21.3	21.3	
M2	0	1.39 ± 0.09	1.66 ± 0.23	1.2	0.683 ± 0.105	15.6 ± 1.2	22.8	19.0	1.09
	0.1	1.45 ± 0.04	1.54 ± 0.08	1.1	0.727 ± 0.088	14.1 ± 0.2	19.4	17.6	
	0.3	1.83 ± 0.09	2.03 ± 0.15	1.1	0.723 ± 0.170	13.4 ± 1.0	18.5	16.8	
	1	1.38 ± 0.13	1.46 ± 0.10	1.1	1.01 ± 0.02	12.1 ± 0.6	12.0	10.9	
	3	1.54 ± 0.11	1.64 ± 0.12	1.1	1.89 ± 0.02	11.0 ± 0.8	5.8	5.3	
	10	1.51 ± 0.11	1.66 ± 0.07	1.1	2.89 ± 0.17	8.40 ± 0.38	2.9	2.6	
	25	1.68 ± 0.05	1.73 ± 0.11	1.0	2.83 ± 0.12	6.19 ± 0.25	2.2	2.2	

A to B: apical to basal, B to A: basal to apical

on CYP2C8 [2], probably because enzalutamide and M2 have the potential to inhibit CYP2C8 and inhibition and induction offset the clinical effect on CYP2C8 substrate exposure. The in vitro determined CYP3A4 induction parameters was calibrated with positive control, rifampicin, and in vitro to in vivo extrapolation of CYP3A4 induction effects were successfully shown in the present analysis.

The prediction of P-gp induction with a PBPK model can be challenging as fundamental physiological information, such as turnover of P-gp in each organ, is sparse and in vitro to in vivo extrapolation of transporter induction has not widely been investigated. As a result, several PBPK works employed a static assumption in P-gp induction by rifampicin [11, 12]. After multiple-dose administration of 600 mg of rifampicin, a 3.5-fold increase in intestinal P-gp expression was determined by Western blot [13], and this value had been used in PBPK analysis of P-gp induction by rifampicin. In contrast, there is a lack of clinical P-gp expression data with other drugs, such as enzalutamide, that have P-gp induction potential in vitro. As enzalutamide showed both P-gp inhibition and induction effects in in vitro studies, a clinical DDI study would only reveal the net effect on P-gp. The clinical net effect of enzalutamide on P-gp was investigated with a typical P-gp substrate, digoxin [3]. Multiple oral administration of 160 mg of enzalutamide increased digoxin AUC and C_{max} by 29% and 17%, respectively, indicating enzalutamide's inhibition effect on P-gp outweighed its induction effect. In this PBPK model analysis, increase in AUC was reproduced with the assumption of no induction on P-gp and use of in vitro P-gp K_i values (Table 4, Fig. 3). Under these assumptions, C_{max} ratio was slightly overpredicted which may be a representation of stronger induction or weaker inhibition of intestinal P-gp in the clinical setting compared to model assumptions. In the clinical study, a decrease in renal clearance of digoxin was observed in the presence of enzalutamide, which may be a result of enzalutamide's inhibitory effect on renal P-gp, which is not accounted for in the present PBPK analysis [3]. Since inhibition of renal P-gp results in an increase in AUC only, not incorporating this mechanism into the model could be a possible reason for overestimation in the C_{max} ratio. Simulations of P-gp induction scenarios (fold increase in P-gp expression of 2.0 or 3.5) were not able to show an increase in digoxin

Table 3 Parameters for enzalutamide and M2 PBPK models

Parameters	Enzalutamide		N-Desmethyl enzalutamide (M2)	
	Value	Assumption(s) and references	Value	Assumption(s) and references
Physicochemical properties and blood binding				
Compound type	Neutral	FDA CP review	Neutral	
Molecular weight	464.44	FDA CP review	450.41	FDA CP review
Log P	2.98	FDA CP review	2.11	In silico calculation with ACD/Labs
B/P ratio	0.55	FDA CP review	0.55	Assumed
f_u	0.0244	FDA CP review	0.0467	FDA CP review
Plasma binding protein	HSA	FDA CP review	HSA	FDA CP review
Absorption				
Absorption model	ADAM		–	
$f_{u,gut}$	0.0244	Assumed to same to f_u	0.0467	Assumed to same to f_u
P_{app} (10^{-6} cm/s) Caco-2 passive permeability (pH6.5:7.5)	31	Internal data	–	
Reference P_{app} (10^{-6} cm/s) Caco-2 passive permeability of propranolol	14.8	Internal data	–	
$P_{eff,man}$ (10^{-4} cm/s)	5.15	Calculated	–	
Formulation	Solution	Assumed	–	
Distribution				
Distribution model	Full PBPK		Minimal PBPK	
Prediction method of V_{ss}	Method 2		Method 1	
V_{ss} (L/kg)	0.967	[1]	0.48	Estimated
K_p scalar	0.933	Optimized	1	
Elimination				
CL_R (L/h)	0	[1]	0	[1]
CYP2C8 CL_{int} for M2 formation (mL/min/pmol enzyme)	0.1518	See text	–	
CYP2C8 CL_{int} for other pathway (mL/min/pmol enzyme)	0.07475	See text	–	
CYP3A4 CL_{int} for M2 formation (mL/min/pmol enzyme)	0.002312	See text	0.001075	See text
CYP3A4 CL_{int} for other pathway (mL/min/pmol enzyme)	0.003617	See text	–	
$CL_{int,HLM}$ (μL/min/mg protein)			1.399	See text
Interaction				
K_i on CYP3A4 (μmol/L)	42	Internal data	–	
K_i on CYP3A5 (μmol/L)	42	Internal data	–	
Ind_{max} on CYP3A4	11.43	See text	9.72	See text
$IndC_{50}$ on CYP3A4 (μmol/L)	1.5	See text	2.5	See text
Ind_{max} on CYP3A5	11.43	Assumed to be same to CYP3A4	9.72	Assumed to be same to CYP3A4
$IndC_{50}$ on CYP3A5 (μmol/L)	1.5	Assumed to be same to CYP3A4	2.5	Assumed to be same to CYP3A4
K_i on P-gp (μmol/L)	1.67	See text	1.09	See text
K_i on OAT3 (μmol/L)	15.1	Internal data	11.5	Internal data

exposure observed in the clinical study unless P-gp K_i values were adjusted from in vitro values (Table 4). A 3.5-fold increase in intestinal P-gp and 5-fold decrease in P-gp

K_i resulted in similar change in digoxin exposure (data not shown). Lack of intestinal P-gp expression change data after multiple doses of enzalutamide prevents us from
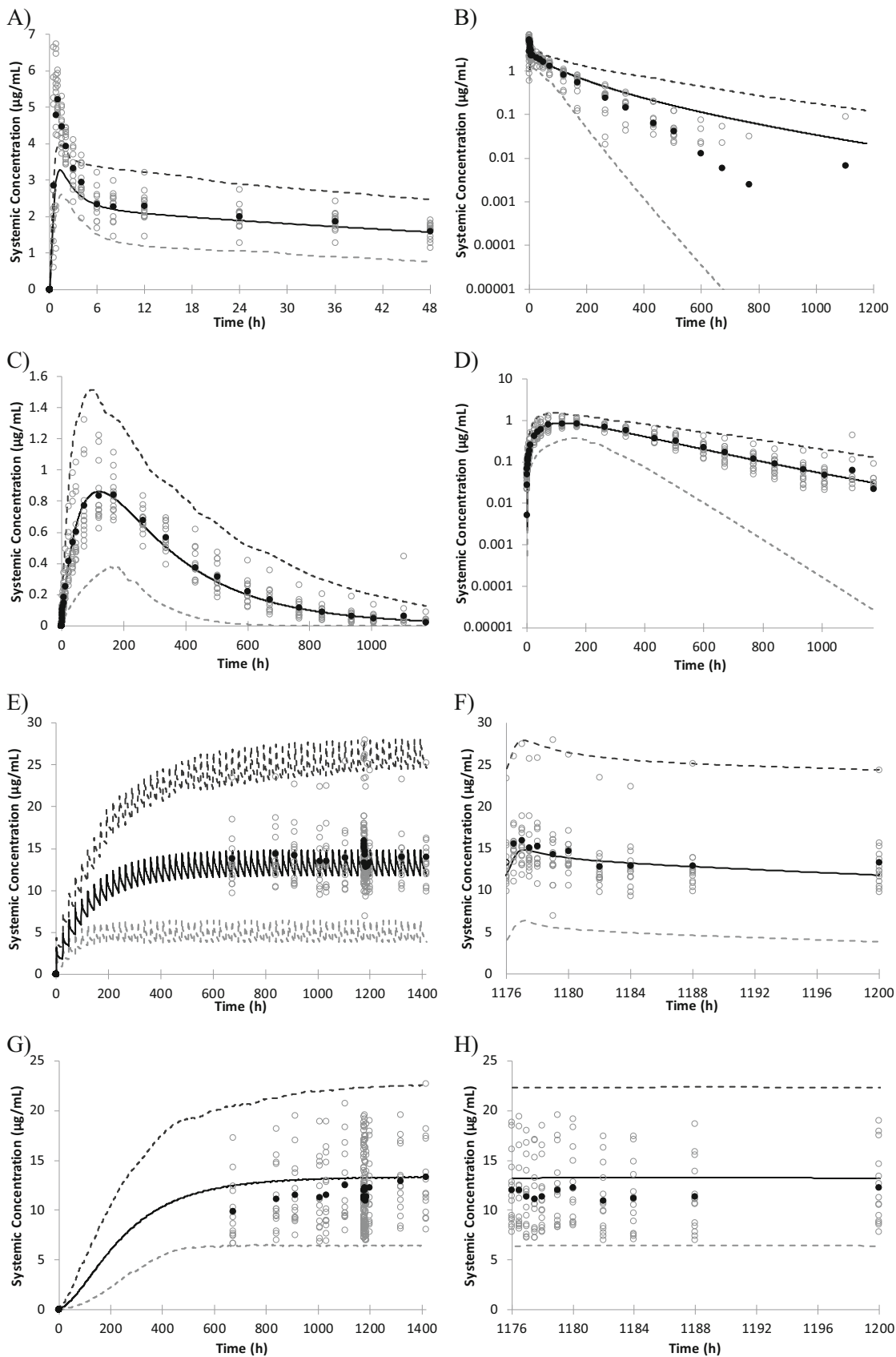
◀**Fig. 1** Observed and simulated plasma concentration–time profiles of enzalutamide and M2: (**A**, **B**) enzalutamide data after single 160 mg dose in linear and semi-log scales; (**C**, **D**) M2 data after single 160 mg dose in linear and semi-log scales; (**E**, **F**) enzalutamide data after multiple 160 mg doses in full-time scale and extracting 1176 to 1200 h; (**G**, **H**) M2 data after multiple 160 mg doses in full-time scale and extracting 1176 to 1200 h. The data shown are simulated mean (solid line), simulated 5th and 95th percentiles (dashed lines), observed mean (filled circles), and observed individual (open circles)

selecting the "true scenario". Instead, we pursued to develop a fit-for-purpose model which can reproduce the net effect on digoxin exposure in presence of enzalutamide.

The developed enzalutamide and M2 PBPK models were applied to the DDI simulation with apixaban and rivaroxaban. The simulation results showed a stronger interaction with rivaroxaban compared to apixaban. This is probably due to two reasons: one is the higher contribution

of CYP3A to rivaroxaban elimination than apixaban, and another is the higher contribution of P-gp to intestinal absorption in apixaban than rivaroxaban. In the model development process of apixaban and rivaroxaban, the contribution of CYP3A to hepatic metabolism was assumed to be 42% and 61%, respectively, and these assumptions were verified with results from many clinical DDI studies using CYP3A inhibitors [10]. In the sensitivity analysis of intestinal P-gp activity, the change in rivaroxaban exposure in the presence of enzalutamide was not affected by intestinal P-gp activity, indicating P-gp does not play an important role in rivaroxaban intestinal absorption. In apixaban, change in intestinal P-gp activity has more impact on apixaban exposure when co-administered with enzalutamide compared to rivaroxaban; however, the impact is still not large. In recent publications, the involvement of intestinal P-gp on apixaban and rivaroxaban absorption was investigated using absorption rates in

Fig. 2 Observed and simulated plasma concentration–time profiles of enzalutamide after (**A**) single and (**B**) multiple doses at several dose levels. The data shown are simulated mean (lines) and observed mean (markers)
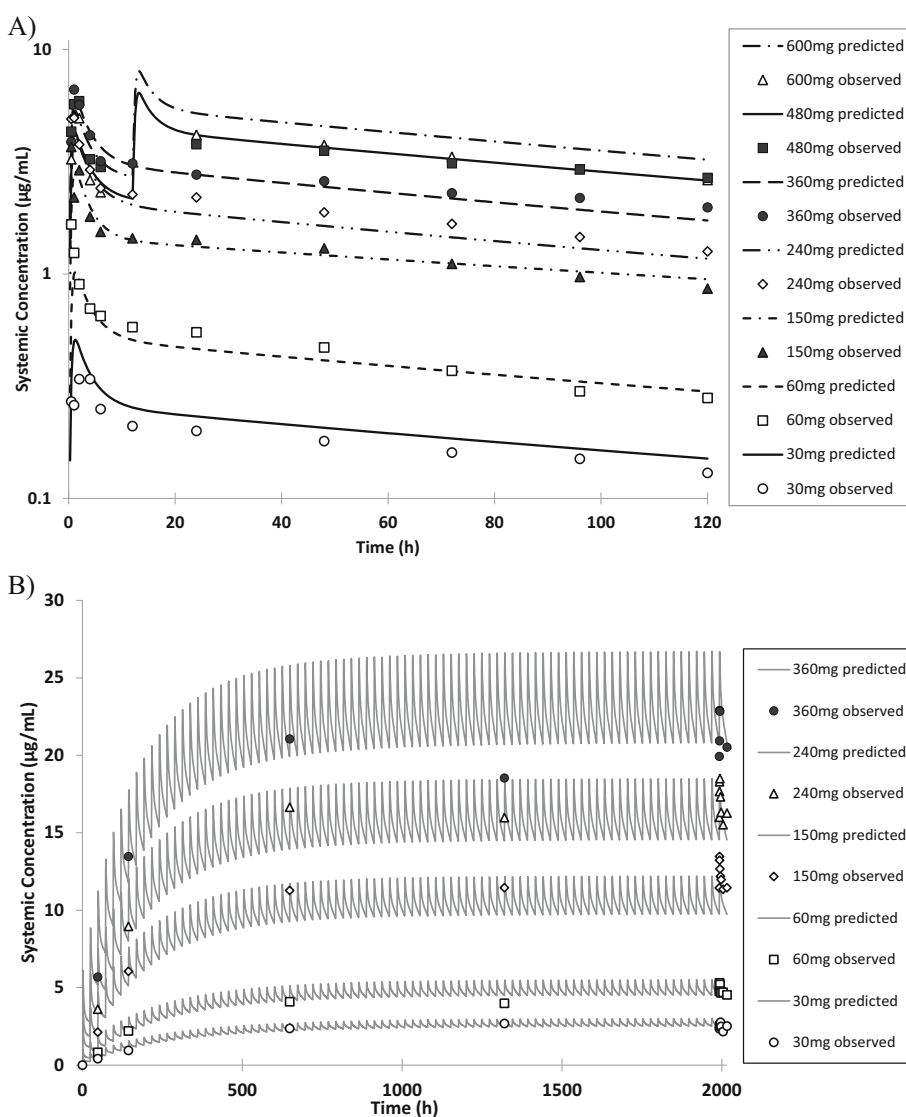
Table 4 Observed and simulated AUC and C_{max} ratios of midazolam and digoxin in presence or absence of multiple 160 mg doses of enzalutamide

		Without enzalutamide		With enzalutamide		AUC ratio	C_{max} ratio
		AUC (ng·h/mL)	C_{max} (ng/mL)	AUC (ng·h/mL)	C_{max} (ng/mL)		
Midazolam							
Observed		32.0 (12.8)	9.98 (3.17)	4.22 (0.784)	2.29 (0.868)	0.14 (0.12–0.17)	0.23 (0.20–0.27)
Simulated		34.4 (24.0)	9.56 (5.93)	4.03 (2.84)	1.91 (1.32)	0.12 (0.11–0.12)	0.19 (0.18–0.20)
Criteria		–	–	–	–	0.07–0.27	0.13–0.42
Digoxin							
Observed		22.1 (4.10)	1.45 (0.314)	28.7 (5.79)	1.69 (0.384)	1.29 (1.21–1.38)	1.17 (1.06–1.29)
Simulated	FI = 1.0	20.0 (6.89)	1.12 (0.322)	25.1 (6.81)	1.54 (0.367)	1.29 (1.19–1.40)	1.38 (1.30–1.47)
	FI = 2.0	20.0 (6.89)	1.12 (0.322)	21.1 (7.11)	1.23 (0.362)	1.06 (0.964–1.16)	1.09 (1.02–1.17)
	FI = 3.5	20.0 (6.89)	1.12 (0.322)	16.5 (7.10)	0.953 (0.341)	0.789 (0.709–0.879)	0.828 (0.767–0.893)
Criteria	–	–	–	–	–	0.91–1.83	0.86–1.59

Data were expressed with mean (SD) for AUC and C_{max} and geometric mean ratio (90% CI) for AUC and C_{max} ratios

Criteria were calculated based on the predictive measure proposed by Guest et al. [20]
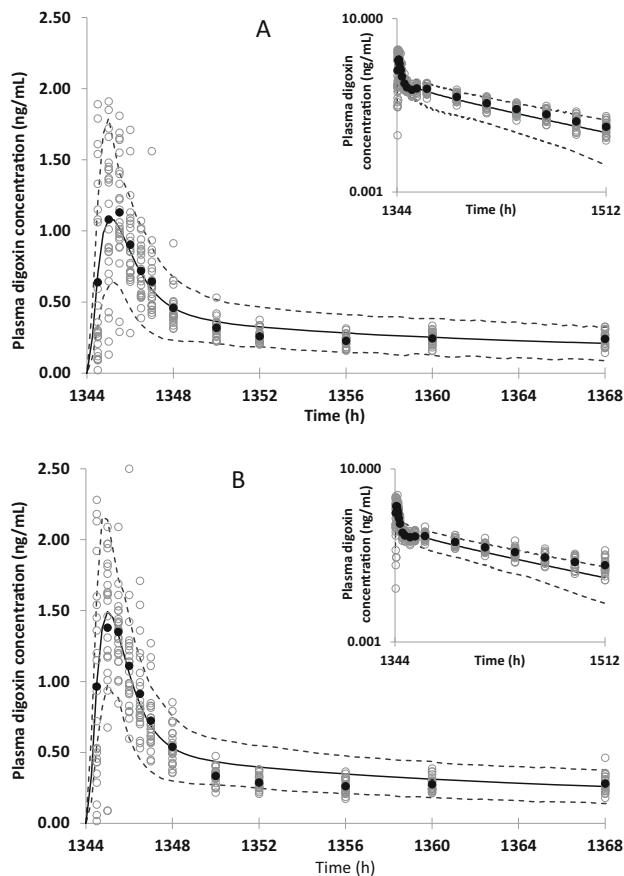
Fig. 3 Observed and simulated plasma concentration–time profiles of digoxin in (**A**) absence and (**B**) presence of enzalutamide. The data shown are simulated mean (solid line), simulated 5th and 95th percentiles (dashed lines), observed mean (filled circles), and observed individual (open circles)

the presence and absence of P-gp inhibitors and inducers as an indicator of P-gp influence in the intestine [14, 15]. The mean absorption time and t_{max} of apixaban and rivaroxaban when concomitantly administered with P-gp inhibitors and inducers suggested limited or absence of effect of efflux transport of apixaban and rivaroxaban by P-gp in the intestine.

For rivaroxaban, two models with different assumptions on renal elimination (low passive permeability and OAT3 involvement or high passive permeability and no OAT3 involvement) were tested. Both enzalutamide and M2 showed OAT3 inhibitory effects in an in vitro study; in vitro K_i values of 15.1 and 11.5 μmol/L, respectively, were incorporated into the models. However, DDI simulation results between Model 1 and Model 2 were similar, and inhibition of OAT3 with enzalutamide and M2 did not result in a substantial change in rivaroxaban plasma exposure.

Rifampicin decreased apixaban and rivaroxaban AUC by 54% and 49%, respectively [16, 17]. The interaction with enzalutamide is estimated to be milder in apixaban (i.e. 31% vs 54%) and mild to similar in rivaroxaban (i.e. 45% vs 49%) compared to rifampicin. Rifampicin also has the potential to inhibit and induce P-gp, even though the clinical DDI study with P-gp substrates indicated rifampicin acts as a P-gp inducer [13]. Multiple oral administration of 600 mg of rifampicin decreased midazolam AUC more than 90% (AUC ratio less than 0.1) [18] and rifampicin's ability to induce CYP3A is considered stronger than that of enzalutamide. Combined with potential net P-gp induction by rifampicin and potential net P-gp inhibition by enzalutamide, the exposure-lowering effect to dual substrates of

Table 5 Simulated AUC and C_{max} ratios of apixaban and rivaroxaban in presence to absence of 160 mg multiple dose of enzalutamide

	Apixaban			Rivaroxaban Model 1		Rivaroxaban Model 2	
	AUC_{inf} ratio	C_{max} ratio		AUC_{last} ratio	C_{max} ratio	AUC_{last} ratio	C_{max} ratio
Population simulation							
GMR (90%CI)	0.691 (0.672–0.709)	1.04 (1.02–1.06)		0.552 (0.535–0.571)	0.746 (0.733–0.758)	0.578 (0.556–0.602)	0.767 (0.752–0.781)
Sensitivity analysis							
Intestinal P-gp RAF/REF			Intestinal P-gp RAF/REF				
2.5	0.651	0.916	0.015	0.561	0.711	0.592	0.740
4.0	0.656	0.930	0.024	0.561	0.713	0.593	0.742
10	0.675	0.980	0.060	0.564	0.719	0.595	0.748
25†	0.711	1.07	0.15†	0.569	0.732	0.601	0.761
100	0.815	1.25	0.60	0.586	0.793	0.619	0.801

RAF/REF: relative activity factor/relative expression factor, †: default RAF/REF setting

P-gp and CYP3A should be stronger in rifampicin than enzalutamide. The present PBPK analysis results support this hypothesis. Rifampicin is defined as a combined P-gp and strong CYP3A inducer, and hence concomitant use with apixaban and rivaroxaban should be avoided per prescribing information of apixaban and rivaroxaban. In contrast, enzalutamide is not a combined P-gp and strong CYP3A inducer, and the exposure change in apixaban and rivaroxaban when concomitantly administered with enzalutamide is estimated to be milder than with rifampicin. Enzalutamide will be concomitantly used with these DOACs. However, a decrease in plasma exposure of apixaban and rivaroxaban based on CYP3A induction was suggested, and care should be taken when apixaban and rivaroxaban are concomitantly administered with enzalutamide.

As for alternative anticoagulant therapy using other DOACs such as dabigatran and edoxaban, both of which are known as P-gp substrates [7], enzalutamide should be concomitantly used with following the instruction for P-gp inhibitors in the labels of these drugs because dabigatran and edoxaban are not substrates of CYP3A and enzalutamide is considered to act simply as a net P-gp inhibitor. Enoxaparin, another DOAC, is not a substrate of P-gp, CYP3A, and other enzymes which enzalutamide may affect, such as CYP2C9 and CYP2C19. Interaction between enzalutamide and enoxaparin is not foreseen.

There are several model limitations. First, there is only one clinical DDI data between enzalutamide and P-gp substrates which prevents extensive verification of enzalutamide and M2 PBPK models as net P-gp inhibitor. P-gp inhibition and induction of the models were calibrated only from one clinical study results, although, preferably, the verification should be conducted with several independent clinical datasets. Second, as a result of challenges in extrapolating in vitro P-gp induction data to in vivo, static assumption in P-gp induction simulation was used. Discrepancy between in vitro and in vivo P-gp inhibition constants had also been reported [19]. For the accurate simulation of net effect on P-gp, robust in vitro to in vivo extrapolation of P-gp inhibition and induction, together with dynamic modeling in PBPK, is needed. Third, the absence of clinical DDI data between enzalutamide and apixaban or rivaroxaban means that the accuracy of the predicted DDI cannot be confirmed. However, based on careful verification of apixaban and rivaroxaban as CYP3A and P-gp substrates [10] and clinical evidence of the potential of enzalutamide as a CYP3A inducer and net P-gp inhibitor, the predicted interaction provides reasonable caution regarding concurrent use of these drugs.

Conclusions

Enzalutamide and M2, a major metabolite of enzalutamide, PBPK models were developed and verified as CYP3A inducers and net P-gp inhibitors by incorporating in vitro determined CYP3A induction data and P-gp inhibition constant to the models. The model predicted possible interaction with apixaban and rivaroxaban when concomitantly administered after 160 mg multiple doses of enzalutamide. Although the predicted decreases in apixaban and rivaroxaban plasma exposure were milder than those observed with rifampicin, concurrent use of these drugs warrants careful monitoring for efficacy and safety.

Declarations

References

1. Gibbons JA, Ouatas T, Krauwinkel W, Ohtsu Y, van der Walt JS, Beddo V, de Vries M, Mordenti J (2015) Clinical pharmacokinetic studies of enzalutamide. Clin Pharmacokinet 54(10):1043–1055. https://doi.org/10.1007/s40262-015-0271-5

2. Gibbons JA, de Vries M, Krauwinkel W, Ohtsu Y, Noukens J, van der Walt JS, Mol R, Mordenti J, Ouatas T (2015) Pharmacokinetic drug interaction studies with enzalutamide. Clin Pharmacokinet 54(10):1057–1069. https://doi.org/10.1007/s40262-015-0283-1

3. Poondru S, Ghicavii V, Khosravan R, Manchandani P, Heo N, Moy S, Wojtkowski T, Patton M, Haas GP (2022) Effect of enzalutamide on PK of P-gp and BCRP substrates in cancer patients: CYP450 induction may not always predict overall effect on transporters. Clin Transl Sci 15(5):1131–1142. https://doi.org/10.1111/cts.13229

4. Gundabolu K (2017) Anticoagulants could be a victim of enzalutamide. J Oncol Pract 13(11):730–731. https://doi.org/10.1200/jop.2017.027615

5. Stevens SM, Woller SC, Kreuziger LB, Bounameaux H, Doerschug K, Geersing GJ et al (2021) Antithrombotic therapy for VTE disease: second update of the CHEST guideline and expert panel report. Chest 160(6):e545–e608. https://doi.org/10.1016/j.chest.2021.07.055

6. Lyman GH, Carrier M, Ay C, Di Nisio M, Hicks LK, Khorana AA et al (2021) American Society of Hematology 2021 guidelines for management of venous thromboembolism: prevention and treatment in patients with cancer. Blood Adv 5(4):927–974. https://doi.org/10.1182/bloodadvances.2020003442

7. Shatzel JJ, Daughety MM, Olson SR, Beer TM, DeLoughery TG (2017) Management of anticoagulation in patients with prostate cancer receiving enzalutamide. J Oncol Pract 13(11):720–727. https://doi.org/10.1200/jop.2017.022004

8. Robertson P, DeCory HH, Madan A, Parkinson A (2000) In vitro inhibition and induction of human hepatic cytochrome P450 enzymes by modafinil. Drug Metab Dispos 28(6):664–671

9. XTANDI®: Clinical Pharmacology and Biopharmaceutics Review(s). https://www.accessdata.fda.gov/drugsatfda_docs/nda/2012/203415Orig1s000ClinPharmR.pdf Accessed 16 Jan 2020

10. Otsuka Y, Choules MP, Bonate PL, Komatsu K (2020) Physiologically-based pharmacokinetic modeling for the prediction of a drug-drug interaction of combined effects on P-glycoprotein and cytochrome P450 3A. CPT Pharmacometrics Syst Pharmacol 9(11):659–669. https://doi.org/10.1002/psp4.12562

11. Neuhoff S, Yeo KR, Barter Z, Jamei M, Turner DB, Rostami-Hodjegan A (2013) Application of permeability-limited physiologically-based pharmacokinetic models: part II - prediction of P-glycoprotein mediated drug-drug interactions with digoxin. J Pharm Sci 102(9):3161–3173. https://doi.org/10.1002/jps.23607

12. Yamazaki S, Costales C, Lazzaro S, Eatemadpour S, Kimoto E, Varma MV (2019) Physiologically-based pharmacokinetic modeling approach to predict rifampin-mediated intestinal P-glycoprotein induction. CPT Pharmacometrics Syst Pharmacol 8(9):634–642. https://doi.org/10.1002/psp4.12458

13. Greiner B, Eichelbaum M, Fritz P, Kreichgauer HP, von Richter O, Zundler J, Kroemer HK (1999) The role of intestinal P-glycoprotein in the interaction of digoxin and rifampin. J Clin Invest 104(2):147–153. https://doi.org/10.1172/jci6663

14. Kou W, Sodhi JK, Wu X, Benet LZ (2021) Investigating intestinal transporter involvement in rivaroxaban disposition through examination of changes in absorption. Pharm Res 38(5):795–801. https://doi.org/10.1007/s11095-021-03039-3

15. Sodhi JK, Liu S, Benet LZ (2020) Intestinal efflux transporters P-gp and BCRP are not clinically relevant in apixaban disposition. Pharm Res 37(10):208. https://doi.org/10.1007/s11095-020-02927-4

16. Vakkalagadda B, Frost C, Byon W, Boyd RA, Wang J, Zhang D, Yu Z, Dias C, Shenker A, LaCreta F (2016) Effect of rifampin on the pharmacokinetics of apixaban, an oral direct inhibitor of factor Xa. Am J Cardiovasc Drugs 16(2):119–127. https://doi.org/10.1007/s40256-015-0157-9

17. XARELTO®: Clinical Pharmacology and Biopharmaceutics Review(s). https://www.accessdata.fda.gov/drugsatfda_docs/nda/2011/022406Orig1s000ClinPharmR.pdf Accessed April 27, 2020.

18. Backman JT, Olkkola KT, Neuvonen PJ (1996) Rifampin drastically reduces plasma concentrations and effects of oral midazolam. Clin Pharmacol Ther 59(1):7–13. https://doi.org/10.1016/s0009-9236(96)90018-1

19. Kimoto E, Vourvahis M, Scialis RJ, Eng H, Rodrigues AD, Varma MVS (2019) Mechanistic evaluation of the complex drug-drug interactions of maraviroc: contribution of cytochrome P450 3A, P-glycoprotein and organic anion transporting polypeptide 1B1. Drug Metab Dispos 47(5):493–503. https://doi.org/10.1124/dmd.118.085241

20. Guest EJ, Aarons L, Houston JB, Rostami-Hodjegan A, Galetin A (2011) Critique of the two-fold measure of prediction success for ratios: application for the assessment of drug-drug interactions. Drug Metab Dispos 39(2):170–173. https://doi.org/10.1124/dmd.110.036103

Publisher's Note Springer Nature remains neutral with regard to jurisdictional claims in published maps and institutional affiliations.